Separation Science and Technology
Publication details, including instructions for authors and subscription information:
http://www.informaworld.com/smpp/title~content=t713708471

Continuum Model Evaluation of the Effect of Saturation on Coalescence Filtration

S. Andan[a]; S. I. Hariharan[a]; G. G. Chase[a]
[a] Microscale Physiochemical Engineering Center, The University of Akron, Akron, OH, USA

To cite this Article Andan, S. , Hariharan, S. I. and Chase, G. G.(2008) 'Continuum Model Evaluation of the Effect of Saturation on Coalescence Filtration', Separation Science and Technology, 43: 8, 1955 — 1973
To link to this Article: DOI: 10.1080/01496390802063630
URL: http://dx.doi.org/10.1080/01496390802063630

Separation Science and Technology, 43: 1955–1973, 2008

ISSN: 0149-6395 print/1520-5754 online
DOI: 10.1080/01496390802063630

Taylor & Francis
Taylor & Francis Group

Continuum Model Evaluation of the Effect of Saturation on Coalescence Filtration

S. Andan, S. I. Hariharan, and G. G. Chase
Microscale Physiochemical Engineering Center,
The University of Akron, Akron, OH, USA

Abstract: Coalescing filters are widely used throughout industry for removal of liquid aerosols from gases or the separation of liquid droplets from emulsions. Typical filters are constructed of non-woven fibers. Fibrous filters are capable of efficient removal of micron and submicron sized droplets and particles. The filtration process is highly complex due to variability in fiber sizes, particle sizes, mixtures of particles and droplets, mixture of types of droplets (oil, water, etc.), and effects of viscosity, surface tension, and chemical reactions between components or with the filter fibers. Prediction of filter performance under such complex conditions is difficult.

Performance of a filter depends on many factors like particle and fiber sizes, flow rate, surface properties of the fibers etc. One of those parameters is the saturation of the filter medium. Saturation is a measure of the amount of liquid present in the void space. Prior models assume that the saturation is uniform along the depth of the medium. In real media, the liquid holdup at steady state need not be uniform with position. Local velocity increases when the saturation is high.

In this paper, a steady state model for a coalescing filter is used to evaluate the effects of saturation on void fraction and its subsequent effect on filter performance. Single fiber mechanisms of direct interception and diffusion deposition are used to model droplet capture efficiencies and drag forces. These mechanisms are applied to volume averaged continuum equations in which the saturation is varied linearly with position in the filter. The results show the minimum pressure drop and largest quality factor occurs with a uniform saturation profile and that variation in average saturation has a greater effect on filter performance than does the slope of the linear saturation profile. The model predicts that uniform saturation profile performs better than the other profiles.

Received 21 September 2007; accepted 11 February 2008.
Address correspondence to G. G. Chase, Microscale Physiochemical Engineering Center, The University of Akron, Akron, OH 44325-3906, USA. Tel: 330-972-7943; E-mail: gchase@uakron.edu

Keywords: Fibrous filters; Saturation; Steady state filtration

INTRODUCTION

Fibrous filters act as a medium to capture droplets from a gas stream. The drops coalesce into bigger droplets and eventually drain out of the filter due to gravity. There are numerous applications of fibrous filters. Fibrous filters are widely used to filter out particles greater than 1 micron diameter (1). They are typically used in metal machining industry to collect airborne liquid droplets generated by the metalworking fluids (2). They are often used inside respirators for cleaning air. They are employed to separate liquid droplets for aerosol sampling and gas cleaning applications (3). These fiber filters can be employed to remove all air borne particles.

Research on fibrous filters gained momentum in late 1950s after the flow fields were determined for flows around arrays of fibers arranged as parallel cylinders (4,5). They used the Stokes equation to simulate the flow field. Kuwabara assumed the same radius and velocity for all cylinders. A statistical approach was used to model the coalescence process and to study the probability of drops in the dispersed phase to collide with drops already on the fibers (6). A model for liquid systems was developed in which droplets from the dispersed phase join the continuous phase due to the concentration gradient (7).

In reference (8) a drop attached to a fiber first grows big and then releases from the fiber due to the capillary and drag forces. Coalescence filtration is described in four stages according to changes in the pressure (9). The pressure drop increases during the first three stages. During the final stage, the pressure drop becomes constant. Also, a comparison is made between the pressure drop profiles of filters with solid and liquid aerosols.

Reference (10) also categorized the coalescence in to four stages: Start-up, loading, unsteady, and steady state processes. The coalescence filtration process is modeled in (11) three steps: approach of a droplet to the fiber, attachment of the droplet, and its release after it grows big. Reference (11) concludes that direct interception is an important mechanism while inertial impaction and diffusion are not as significant. Prior works describe pressure drop profiles when the liquid hold up varies. Not much work has been done to determine the actual hold-up of liquid as a function of position in the medium at steady state.

Saturation is defined as the ratio between the volume fraction of the liquid and the porosity of the filter medium. It is a measure of the amount of liquid present in the void space. In solid aerosol filtration, the pressure drop continually increases with solids loading in the filter (9). In the

filtration of liquid aerosols, the pressure drop initially increases and then becomes constant when the system reaches steady state. At steady state, the liquid drainage becomes equal to the loading rate. The local saturation of the dispersed phase was measured by joining different layers of filter media together (12). The saturation was largest at the entrance, minimum in the interior, and a smaller increase at the exit. A different saturation profile was reported (13) in which the saturation is uniform except near the exit where it increases slightly. The saturation was observed to decrease as the flow velocity increased (14). Assumed a uniform saturations of 10% were used to predict the performance of the filters with variation in fiber size (15).

A theoretical model is applied to investigate how the saturation profile affects the filter pressure drop and efficiency, with microfiber filter media. In this work the saturation is modeled as linearly varying with the filter depth, having a slope (m) and intercept (b). The effects of different slopes and intercepts on the filter performance can be calculated through its effect on filter porosity. This model does not tell us how to obtain the specified saturation profiles. The unsteady performance of the filter must be modeled to predict the steady state saturation profile which is beyond the scope of the present work.

ASSUMPTIONS

Volume averaged continuum equations are used to model the coalescing filter performance. The complete sets of equations are complicated and cannot be solved analytically. The following assumptions simplify the equations to obtain a tractable solution:

1. Media fibers are rigid and stationary.
2. Droplets are spherical.
3. The media is incompressible.
4. Isothermal process.
5. Unidirectional flow in z direction.
6. The liquid droplets are captured by the fibers. Capture of droplets by other droplets on the fibers or by the binder material is neglected.
7. The porosity of the filter media is uniform and isotropic.
8. Binder material (i.e. glue) accounts for only a small fraction of the filter volume and can be neglected.
9. The coalesced droplets do not re-entrain into the air stream.
10. The concentration of liquid droplets in the inlet stream is low enough to assume the bulk density of inlet air stream is equal to density of air at that temperature.

11. Diffusion is negligible and there are no chemical reactions.
12. Inertial terms and air drag on the filter housing walls are negligible compared to the pressure gradient and drag on the fibers in the momentum equation.
13. Saturation is a linear function of dimensionless position

$$S = m\frac{z}{L} + b \tag{1}$$

Here m = slope and b = Intercept of the linear saturation profile.

CONSERVATION EQUATIONS

The volume averaged conservation equations (16) are used to calculate the pressure drop, outlet concentration and quality factor. Only the gas phase species balance and the gas phase momentum balance are needed. Applying the assumptions, the relevant continuum equations reduce to:

Gas Phase Oil Species Balance

$$\frac{\partial(\varepsilon^G \rho_0^G v_z^G)}{\partial z} + I_0^G = 0 \tag{2}$$

Gas Phase Momentum Balance (z Component)

$$\varepsilon^G \frac{\partial P}{\partial z} + F_z^G = 0 \tag{3}$$

The filter porosity ε is defined as the void volume fraction (*i.*e., void volume/filter volume). The liquid and gas phase volume fractions are similarly defined as ε^L and ε^G (phase volume/filter volume). The porosity is related to phase volume fractions by

$$\varepsilon = \varepsilon^L + \varepsilon^G \tag{4}$$

The saturation, S, quantifies how much of void space is filled with liquid and is related to porosity and liquid volume fraction by

$$\varepsilon^L = S\varepsilon \tag{5}$$

Similarly, the gas volume fraction is related to saturation by

$$\varepsilon^G = (1 - S)\varepsilon \tag{6}$$

The mass fraction of oil in gas phase is the ratio of the oil mass concentration to the gas phase density by

$$w_0^G = \frac{\rho_0^G}{\rho^G} \tag{7}$$

Rewriting the species and momentum equations with help of Eqs. (4) through (7) we get

Species Balance

$$\frac{\partial\left((1-S)\varepsilon w_0^G \rho^G v_z^G\right)}{\partial z} + I_0^G = 0 \tag{8}$$

Momentum Balance

$$(1-S)\varepsilon \frac{\partial P}{\partial z} + F_z^G = 0 \tag{9}$$

The momentum balance is solved by introducing a constitutive relation for the drag force. The species balance is solved by introducing a constitutive equation for the mass transfer term I_0^G.

PARTICLE CAPTURE MECHANISMS

The mass transfer term for the oil leaving the gas phase is related to the filter coefficient, α by

$$I_0^G = \alpha \rho_0^G \varepsilon^G v_z^G \tag{10}$$

$$\text{where } \alpha = E\alpha_f \tag{11}$$

$$\alpha_f = \frac{4(1-\varepsilon)}{\pi d_f} \tag{12}$$

Here, E is the single fiber efficiency and $\alpha_{100\%}$ is the filter coefficient for a 100% capture efficiency based on the projected area of the fiber.

Particles in the air may be captured by several mechanisms including direct interception, inertial impaction, diffusional deposition, gravitational deposition, or electrostatic forces (17). All of the mechanisms apply simultaneously, though one mechanism may dominate over the others depending on the particle size, the filter media, and the gas flow conditions. The capture mechanisms in turn are related to the single fiber efficiency in Eq. (11). In this work direct interception and diffusional

deposition are dominant due to the size of the droplets involved. The other mechanisms are not considered. Hence $E = E_{DR}$.

Interception and Diffusion

Following are the equations used to determine the single fiber efficiency under continuum and slip flow conditions (8). The capture of micron sized droplets is assumed to be adequately modeled by mechanisms for capture of similar sized solid particles on dry fibers.

Continuum Flow

$$E_{DR} = \frac{4}{\zeta d_f^2}\left[\frac{3D\zeta d_f^2\pi}{8v_z} + \left(\frac{d_p}{2}\right)^2\right]^{2/3} \tag{13}$$

where ζ is the hydrodynamic factor given by

$$\zeta = \left(-\frac{1}{2}\ln(1-\varepsilon) - 0.75\right) \tag{14}$$

Slip Flow

$$E_{DR} = E_D + E_R + E'_{DR}(Pe, N_R) \tag{15}$$

$$E'_{DR}(Pe, N_R) = 1.24\zeta'^{(-0.5)}Pe^{(-0.5)}N_R^{2/3} \tag{16}$$

$$\zeta' = -0.5\ln(1-\varepsilon) - 0.52 + 0.64(1-\varepsilon) + 1.43\varepsilon Kn \tag{17}$$

Here, ζ' is the hydrodynamic factor, including the effect of aerodynamic slip (17), N_R is the diameter ratio, Kn is the Knudsen number, Pe is the Peclet number, and D is the diffusivity, given by

$$N_R = \frac{d_p}{d_f} \tag{18}$$

$$Kn = \frac{2\lambda}{d_f} \tag{19}$$

$$Pe = \frac{v_z^G d_f}{D} \tag{20}$$

$$D = \mu k_B T \tag{21}$$

$$\mu = \frac{Cn}{3\pi\eta d_p} \tag{22}$$

$$Cn = 1 + \frac{2A\lambda}{d_p} + \frac{2Q\lambda}{d_p}\exp\left(\frac{Bd_p}{2\lambda}\right) \tag{23}$$

Here, Cn is the Cunningham factor, k_B is Boltzmann's constant (1.38066×10^{-23} J/°K), $\lambda = 0.065\,\mu$m is the free path of molecules at STP, and the remaining parameters are constants ($A = 1.246$, $Q = 0.42$, and $B = 0.87$).

Direct Interception

For microfibers the single fiber efficiency due to direct interception can be estimated by the following expression (17).

$$E_R = \frac{1}{2\zeta'}\Big\{2(1+N_R)\ln(1+N_R) + (1+N_R)^{-1} - (1+N_R) + 2.86\,Kn(2+N_R)N_R(1+N_R)^{-1}\Big\} \tag{24}$$

Diffusional Deposition

The single fiber efficiency for Diffusional Deposition acting alone is given by (17)

$$E_D = 2.7Pe^{(-2/3)}\left[1 + 0.39\zeta'^{(1/3)}Pe^{(-1/3)}Kn\right] \tag{25}$$

CALCULATION OF DRAG FORCE AND PRESSURE DROP

Many correlations relating pressure drop to fiber size in filter media are developed as macroscopic expressions. We can apply these expressions to a differential volume and then let the differential volume thickness become infinitesimal to deduce an expression for the drag force in Eq. (9).

We define the force per unit length of fiber as f_f for a fiber of diameter d_f. The pressure drop is related to the force per unit length of fiber by

$$A\Delta P = L_f f_f \tag{26}$$

For a uniform drag force, Eq. (9) integrated over filter of thickness L gives

$$F_z^G = (1 - S)\varepsilon \frac{\Delta P}{L} \tag{27}$$

Hence

$$F_z^G = (1 - S)\varepsilon \frac{L_f f_f}{AL} \tag{28}$$

Let ε_f represent the volume fraction of the filter occupied by the fibers of diameter d_f and total length L_f. Then

$$\varepsilon_f = \frac{V_f}{AL} \tag{29}$$

where L is the filter thickness. The volume occupied by the fibers of diameter d_f is

$$V_f = \frac{\pi d_f^2 L_f}{4} \tag{30}$$

Hence the volume fraction occupied by the fibers is

$$\varepsilon_f = \frac{\pi d_f^2 L_f}{4AL} \tag{31}$$

Therefore, the length of the fiber of size d_f is given by

$$L_f = \frac{4AL\varepsilon_f}{\pi d_f^2} \tag{32}$$

Substitution of Eq. (32) into (28) gives the drag force F_z^G as

$$F_z^G = (1 - S)\varepsilon \frac{4\varepsilon_f}{\pi d_f^2} f_f \tag{33}$$

We allow the drag force in (33) to apply to a small differential element of a filter. In the limit as the differential element size becomes infinitesimal then (33) can be applied in Eq. (9) to obtain

$$\frac{\partial P}{\partial z} + \frac{4\varepsilon_f}{\pi d_f^2} f_f = 0 \tag{34}$$

For uniform properties Eq. (34) gives an expression to determine drag force per unit length of fiber from macro scale correlations

$$f_f = -\frac{\Delta P}{L}\frac{\pi d_f^2}{4\varepsilon_f} \tag{35}$$

For $Kn < 0.25$ (slip flow), reference (17) provides a correlation for the pressure drop to be

$$\Delta P = \frac{16\mu\varepsilon_f L v_z^G (1 + 1.996Kn)}{d_f^2 \left[\begin{array}{l} (-0.5\ln(\varepsilon_f) - 0.75 + \varepsilon_f - \dfrac{\varepsilon_f^2}{4} \\ \quad + 1.996Kn\left(-0.5\ln(\varepsilon_f) - 0.25 + \dfrac{\varepsilon_f^2}{4}\right) \end{array} \right]} \tag{36}$$

Equation (36) was derived using the Kuwabara approach (18). This model assumes that the aerosol droplets are captured on the fiber through the diffusion mechanism. This pressure drop model was based on experimental results (19). The equation was derived for spherical particles. From Eq. (35), we obtain the expression for f_f to be

$$f_f = -\frac{4\mu\pi(1 - S)v_Z^G(1 + 1.996Kn)}{\left[\begin{array}{l} (-0.5\ln(\varepsilon_f) - 0.75 + \varepsilon_f \\ \quad - \dfrac{\varepsilon_f^2}{4} + 1.996Kn\left(-0.5\ln(\varepsilon_f) - 0.25 + \dfrac{\varepsilon_f^2}{4}\right) \end{array} \right]} \tag{37}$$

Substituting Eqs. (37) and (1) in (34) and integrating from $z = 0$ to $z = L$, gives

$$\frac{\Delta P}{L} = \left(\frac{16\mu\varepsilon_f Q(1 + 1.996Kn)}{d_f^2 \left[\begin{array}{l} (-0.5\ln(\varepsilon_f) - 0.75 + \varepsilon_f - \dfrac{\varepsilon_f^2}{4} \\ \quad + 1.996Kn\left(-0.5\ln(\varepsilon_f) - 0.25 + \dfrac{\varepsilon_f^2}{4}\right) \end{array} \right]} \right) \times \left(\frac{1}{A\varepsilon m} \ln\left(\frac{(1 - b)}{(1 - \frac{m}{L}z - b)} \right) \right) \tag{38}$$

where

$$v_z = \frac{Q/A}{\varepsilon(1-S)} \tag{39}$$

which gives an expression that accounts for the assumed linear saturation profile.

For $Kn < 0.01$ (Continuum flow), from reference (17), we get a correlation for the pressure drop to be

$$\Delta P = \frac{16\mu\varepsilon_f L v_z^G}{d_f^2\left[(-0.5\ln(\varepsilon_f) - 0.75 + \varepsilon_f - \frac{\varepsilon_f^2}{4}\right]} \tag{40}$$

By Eq. (35) we derive the expression for f_f to be

$$f_f = -\frac{4\mu\pi v_z^G}{\left[(-0.5\ln(\varepsilon_f) - 0.75 + \varepsilon_f - \frac{\varepsilon_f^2}{4}\right]} \tag{41}$$

Substituting Eqs. (41) and (1) in (34) and integrating from $z = 0$ to $z = L$, gives

$$\frac{\Delta P}{L} = \frac{16\mu\varepsilon_f Q}{d_f^2\left[(-0.5\ln(\varepsilon_f) - 0.75 + \varepsilon_f - \frac{\varepsilon_f^2}{4}\right] A\varepsilon m \ln\left(\frac{(1-b)}{(1-\frac{m}{L}z-b)}\right)} \tag{42}$$

Equations (38) and (42) are used to calculate the pressure drop for slip and continuum flow conditions for varying values of m and b.

CALCULATION OF OUTLET CONCENTRATION

Combining Eqs. (6), (7) and (10) into (8), the species balance is written as

$$\frac{d}{dz}((1-S)\varepsilon\rho^G w_0^G v_z^G) = -\alpha(1-S)\varepsilon\rho^G w_0^G v_z^G \tag{43}$$

The relationship between the gas velocity v_z^G and the bed saturation to the gas flow rate is given by

$$v_z = \frac{Q/A}{\varepsilon(1-S)} \tag{44}$$

On integrating equation (43) using equation (44) where Q is a constant yields,

$$\ln\left(\frac{w_0^G(L)}{w_0^G(0)}\right) = \left(-\int_0^L \alpha dz\right) \tag{45}$$

Here α is a function of saturation which in turn is a function of z. Hence, the right hand side integral in Eq. (45) is evaluated numerically using trapezoidal rule of integration. Let "a" be the value of the integral, then the outlet mass fraction is given by

$$\frac{w_{OUT}}{w_{IN}} = \exp(-a) \tag{46}$$

DETERMINATION OF QUALITY FACTOR

Quality factor (QF) is defined by (8)

$$QF = \frac{-\ln\left(\frac{w_{OUT}}{w_{IN}}\right)}{\Delta P} \tag{47}$$

Substitution of Eq. (46) gives the expression for QF as

$$QF = \frac{a}{\Delta P} \tag{48}$$

RESULTS

The model was programmed using MS-EXCEL and the results are shown in the plots described below. The model parameters were $d_f = 4$ microns, $d_p = 1$ micron, and $L = 0.01\,m$.

Figures 1 through 8 show how the variations in saturation effect pressure drop, quality factor, and outlet mass fraction with different average saturation and different uniform saturation levels.

Figures 1–3 are for different saturation slopes for media with average saturations of 0.1 and 0.2. Figures 4–6 are for uniform saturation where $m = 0$. Figure 7 shows local variations in pressure for different slopes and intercepts. Figure 8 shows local variations in pressure for uniform saturations.

Average saturations in laboratory filters at steady state are typically in the range of 0.1–0.2. These values are applied in this work. When $m \neq 0$, the average saturation is related to the intercept, b by

$$S_{avg} = 0.5\,m + b \tag{50}$$

Since b can not be negative then m is restricted to the range of $-2S_{avg} \leq m \leq +2S_{avg}$.

DISCUSSION OF RESULTS

Figures 1–3 show the quality factor, pressure drop, and outlet mass fraction as a function of different slopes for saturation line for average saturations 0.1 and 0.2. These figures show that the pressure drop is least at zero slope. The pressure drop increases with magnitude of the saturation slope. The outlet concentration also increases with magnitude of the slope with the smallest outlet configuration occurring at $m = 0$. The quality factor is largest at $m = 0$, consistent with the trends in pressure and concentration. In Figs. 1–3, there is symmetry between the parameter values with the same positive and negative slopes. When there is a positive slope, the pressure decreases slowly from the entrance to the mid section of the filter and decreases significantly from the middle to the exit. When the slope is negative, the opposite effect occurs which creates symmetry around the average saturation. The plots show that the average saturation has a greater effect on pressure, concentration, and quality factor than does the slope. Changing the slope from 0 to 0.4 causes 2% change in $\frac{\Delta P}{L}$ whereas a change in average saturation from 0.2 to 0.1 causes a 13% change.

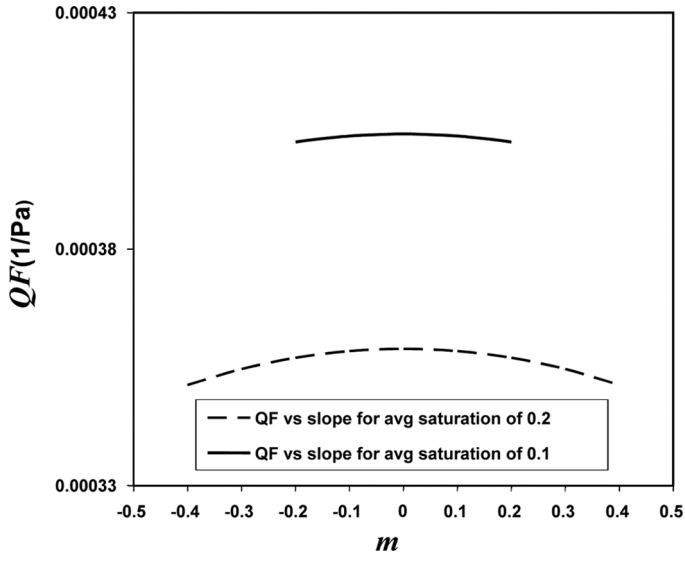

Figure 1. Quality Factor for different slopes, m, of the saturation profile.

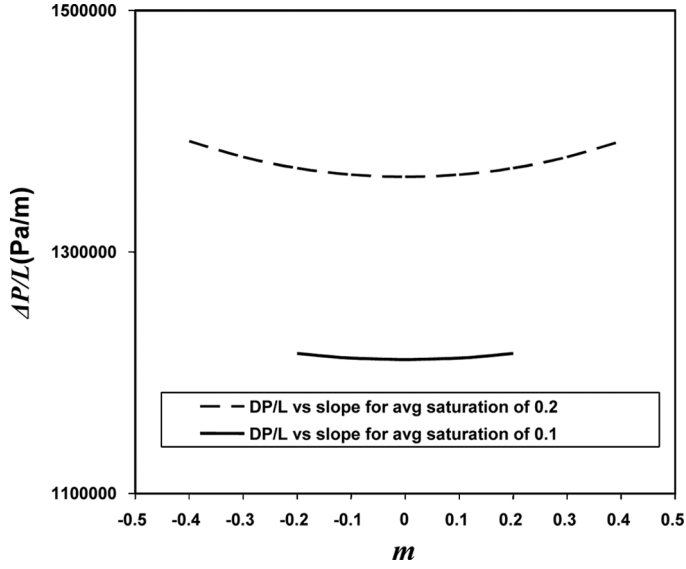

Figure 2. $\frac{\Delta P}{L}$ for different slopes of saturation line.

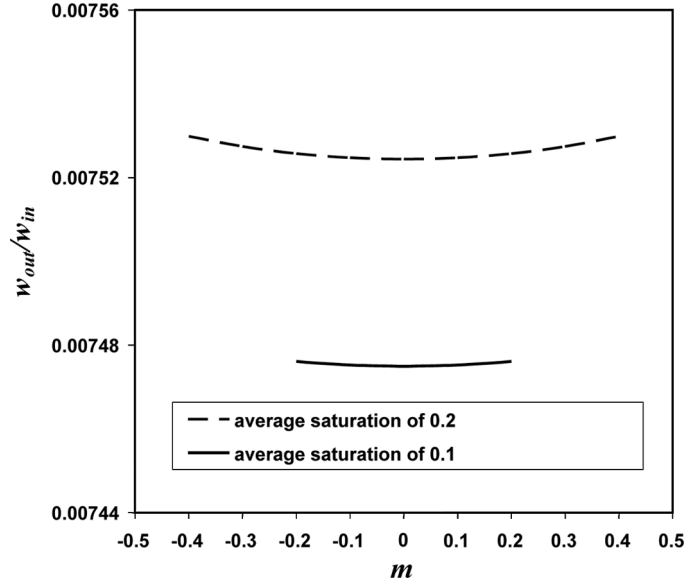

Figure 3. $\frac{w_{out}}{w_{in}}$ for different slopes of saturation line.

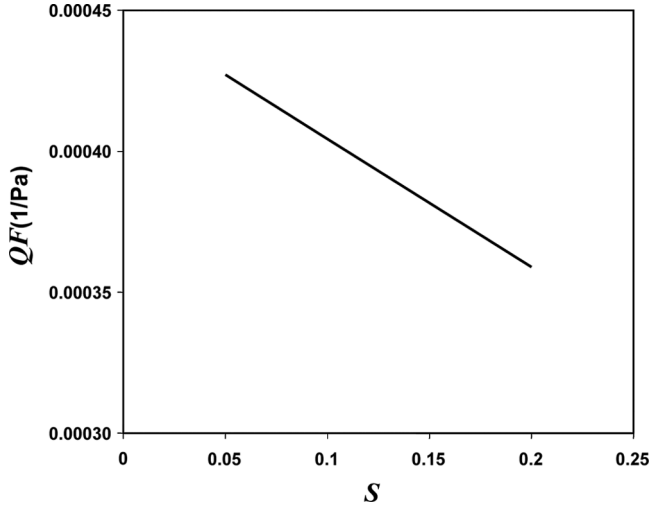

Figure 4. Quality Factor for different uniform saturations for $m = 0$.

Figures 4–6 assume uniform saturation and show the effects of saturation on the quality factor, pressure drop, and the outlet concentration. The pressure drop increases when the saturation increases. When the saturation is high, the area available for fluid flow is restricted, causing

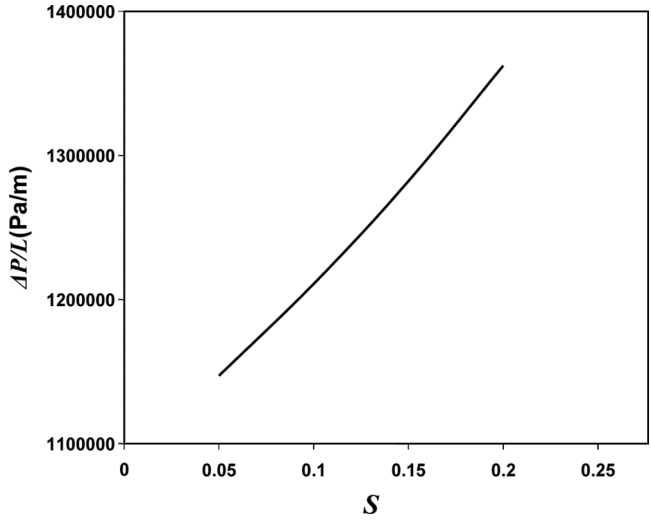

Figure 5. Pressure drop for different uniform saturation for $m = 0$.

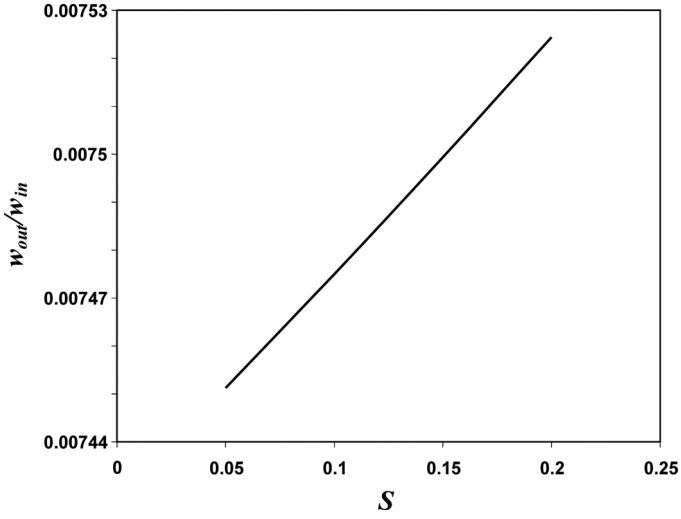

Figure 6. $\frac{w_{out}}{w_{in}}$ for different uniform saturations for $m = 0$.

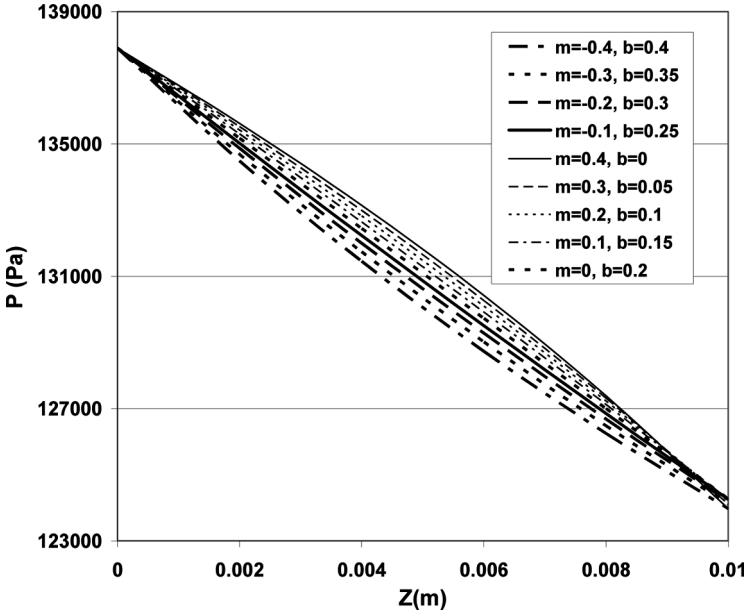

Figure 7. Local pressure at different positions in the bed for different saturation lines of average saturation of 0.2.

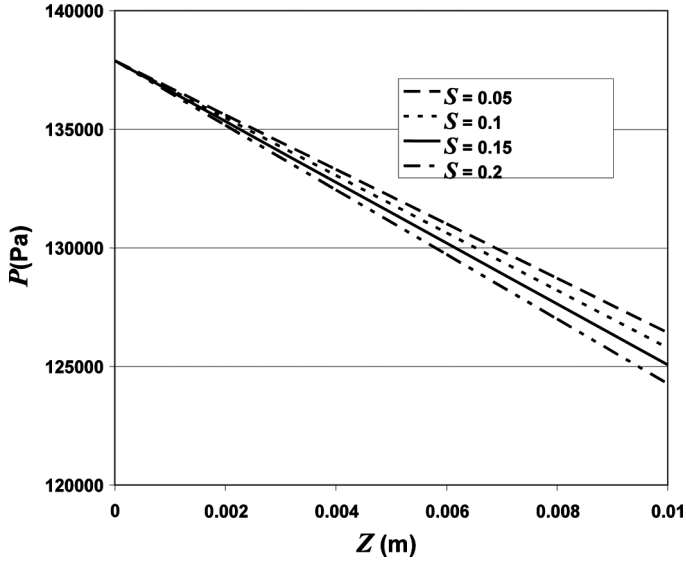

Figure 8. Local pressure at different positions in the bed for different uniform saturations for $m = 0$.

a larger interstitial velocity which causes the pressure drop to increase. Corresponding to the pressure drop, the quality factor decreases as saturation increases.

Figure 7 shows the pressure as a function of position for different saturation lines of average saturation of 0.2. This plot shows how the pressure changes inside of the medium as a function of position. For higher positive slopes of the saturation line, initially the pressure decreases slowly with position and decreases rapidly near the exit. For negative slopes, the opposite occurs. When the slope is positive, the inlet saturation is lower than the exit saturation. Less liquid holdup at the inlet offers less resistance to air flow and the corresponding pressure decrease is small. Increasing saturation along the filter depth increases the resistance to airflow with a corresponding increase in pressure gradient. For a uniform saturation profile, the pressure drops linearly with position.

Figure 8 shows the pressure as a function of position for different constant saturation lines. As expected, this plot clearly shows that the pressure drop is smaller for media with lower saturations at steady state.

The uniform saturation profile was found to be the optimum saturation profile at which the values of the filtration parameters are optimum. Non-uniform saturation profiles cause an increase in pressure drop and decrease in quality factor.

CONCLUSIONS

The model results on coalescence filtration at steady state condition show that the pressure drop is lowest and quality factor is highest when the saturation profile is uniform. The results also show variation in average saturation has a greater effect on the filter performance than does the slope of the linear saturation profile.

The model developed here is based on volume averaged continuum theory. The model does not predict how to obtain the particular saturation profiles but it does show the filter performances. Predictions of particular saturation profiles are beyond the scope of this work.

NOTATION

A: *Filter* Area
b: Intercept of the saturation line
Cn: Cunningham factor
D: Coefficient of diffusion
d_f: fiber diameter
d_p: Diameter of the droplet
E: Convective transport of property ϕ across an interphase boundary
E_D: Single fiber efficiency by diffusion
E_R: Single fiber efficiency by Direct Interception
E_{DR}: Overall Single Fiber Efficiency due to interception and diffusion
$\underline{F}_z^G$: Drag force of the moving gas on the fibers
f_f: Drag force per unit length of fiber of diameter d_f
I_o^G: mass flux of particle captured by the fibers from the gas phase
Kn: Knudsen number
Ku: Kuwabara number
L: thickness of media
m: slope of the linear saturation profile
N_R: interception parameter
Pe: Peclet number
ΔP: Pressure drop
Q: Volumetric flow rate
QF: Quality Factor
S_{avg}: Average saturation
St: Stokes number
v_0: Approach velocity of air
$\underline{v_Z^G}$: gas phase interstitial velocity
$\overline{V_f}$: Volume of micro fiber
w_0^G: Mass fraction of oil in gas phase

α: Filter Coefficient
α_f: Filter Coefficient of a 100% efficient fiber of diameter d_f
ε: porosity of the media
ζ: Hydrodynamic factor
ζ': Hydrodynamic factor, including aerodynamic slip
λ: mean free path
ρ^G: Gas phase density
ρ_O^G: mass concentration of oil droplet in the gas phase

ACKNOWLEDGEMENT

This work was supported by the Coalescence Filtration Nanomaterials Consortium: Ahlstrom Paper Group, Donaldson Company, Cummins Filtration, Hollingsworth and Vose, and Parker Hannifin.

REFERENCES

1. Destephen, J.A., Choi, K.J. (1996) Modeling of filtration processes of fibrous filter media. *Separations Technology*, *6*: 55.
2. Leith, David; Leith, Frank A., Boundy, Maryanne G. (1996) Laboratory measurements of oil mist concentrations using filters and an electrostatic precipitator. *American Industrial Hygiene Association Journal*, *57* (12): 1137–1141.
3. Raynor, Peter C., Leith, David. (1999) The influence of accumulated liquid on fibrous filter performance. *Journal of Aerosol Science*, *31* (1): 19–34.
4. Kuwabara, S. (1959) The forces experienced by randomly distributed parallel circular cylinders or spheres in a viscous flow at small reynolds number. *Journal of the Physical Society of Japan*, *14* (4): 527.
5. Happel, J. (1959) Viscous flow relative to arrays of cylinders. *AICHE J.*, *5*: 174.
6. Sherony, D.E., Kintner, R.C., Wasan, D.T. (1978) Coalescence of secondary emulsions in fibrous bed. *Surface Colloid Science*, *10*: 99.
7. Spielman, L.A., Goren, S.L. (1972) Theory of coalescence by flow through porous media. *Ind. Eng. Chem. Fundam.*, *11*: 66.
8. Rosenfeld, J.I., Wasan, D.T. (1974) Coalescence of drops in a liquid-liquid dispersion by passage through a fibrous bed. *Can. J. Chem. Eng.*, *52*: 3.
9. Walsh, D.C., Stenhouse, J.I., Scurrah, K.L., Graef, A. (1996) The effect of solid and liquid aerosol loading on fibrous filter material performance. *Journal of Aerosol Science*, *27*: 5617.
10. Vasudevan, G., Shin, C.G., Raber, B., Suthar, A., Chase, G.G. (2002) Modeling the start-up stage of coalescence filtration. *Fluid/Particle Separation Journal*, *14* (3): 169.

11. Hazlett, R.N. (1969) Fibrous bed coalescence of water. *Industrial & Engineering Chemistry Fundamentals*, *8* (4): 625.
12. Bitten, J.F., Fochtman, E.G. (1971) Water distribution in fiber-bed coalescers. *Journal of Colloid and Interface Science*, *37* (2): 312.
13. Richardson, J.G., Kerver, J.L., Hafford, J. A., Osaba, J. (1952) Laboratory measurements of relative permeability. *Trans. AIME*, *195*: 187.
14. Contal, P., Simao, J., Thomas, D., Frising, T., Calle, S., Collin, J. C., Bemer, D. (2004) Clogging of fibre filters by submicron droplets. Phenomena and influence of operating conditions. *Aerosol Science*, *35*: 263.
15. Srinivasan, P., Chase, G.G. (April 2005) Steady state filter media performance modeling with and without nanofibers. *American Filtration and Separations Society*, 18th Annual Conference. Atlanta.
16. Chase, G.G. (2002) Transport phenomena in porous media, in *Fluid Flow Handbook*, Saleh, J. Ed.; Chapter 21, McGraw-Hill: New York.
17. Borwn, R.C. (1993) *Air Filtration : An Integrated Approach to the Theory and Applications of Fibrous Filters*; Pergamon Press.
18. Pich, J. (1971) Pressure characteristics of fibrous aerosol filters. *Journal of Colloid & Interface Science*, *37*: 912.
19. Stern, S.C., Zeller, H.W., Schekman, A.I. (1952) The aerosol efficiency and pressure drop of a fibrous filter at reduced pressures. *Journal of Colloid Science*, *15*: 546.